Measurement xxx (2016) xxx–xxx

Contents lists available at ScienceDirect

Measurement

journal homepage: www.elsevier.com/locate/measurement

An investigation of accuracy, repeatability and reproducibility of laser micromachining systems

Debajyoti Bhaduri *, Pavel Penchev, Stefan Dimov, Sein Leung Soo

Department of Mechanical Engineering, School of Engineering, The University of Birmingham, Edgbaston, Birmingham B15 2TT, UK

ARTICLE INFO

Article history:
Received 7 December 2015
Received in revised form 10 March 2016
Accepted 14 March 2016
Available online xxxx

Keywords:
Laser micro machining
Accuracy
Repeatability
Reproducibility
Uncertainty
Precision metrology

ABSTRACT

Component technologies of laser micro machining systems are the key factors affecting their overall performance. The effects of these technologies on accuracy, repeatability and reproducibility (ARR) in different implementations of such systems have to be investigated to quantify their contributions to the overall processing uncertainty, especially those with the highest impact on beam delivery sub-systems. The aim of this research was to evaluate the capabilities of state-of-the-art machining platforms that were specially designed and implemented for laser micro structuring and texturing. An empirical comparative study was conducted to quantify the effects of key component technologies on ARR of four state-of-the-art systems. In particular, the capabilities of the optical and mechanical axes were investigated when they were utilised separately or in combination for precision laser machining. Conclusions are made about the positional accuracy of the mechanical and optical axes and the importance of their proper calibration on the systems' overall performance is discussed. It is shown that the laser machining platforms can achieve repeatability and reproducibility better than 2 µm and 6 µm, respectively.

1. Introduction

Laser surface structuring and texturing of mechanical parts attracted a lot of interest from the tribological community recently [1] as it offers a great potential to improve significantly the frictional characteristics of mechanical components [2] and also to lead to more energy efficient mechanical systems [3]. The technology was further applied successfully for producing micro structures and surface textures on miniaturised parts [4], particularly in the fields of biomedicine, microelectronics, telecommunication, aerospace, automotive and micro-injection moulding [5,6]. Laser surface texturing, mainly with dimples and micro-pits on different substrate materials, was reported by many research groups, e.g. on silicon and TiO_2 with excimer lasers [6], and 100Cr6 steel [7], T8 steel [8], stainless steel [9] and Ti–6Al–4V [10] with Nd:YAG lasers.

Although laser structuring and texturing have attracted the attention of research communities and industry as emerging viable processes for surface functionalisation and micro-manufacturing, their implementation in practice requires high precision machining platforms. The beam delivery sub-systems of such laser micromachining platforms, especially their key component technologies, determine their ARR capabilities to a great extent and therefore have to be investigated systematically in order to quantify their contributions and effects on the overall process uncertainty. Such a research has to be conducted by utilising appropriate metrology methods with the necessary capabilities for inspecting features/structures at sub-micron scale. One of the methods that can offer a solution to such complex characterisation tasks is the Focus Variation (FV) technology [11]. In particular, FV systems

* Corresponding author.
E-mail addresses: debajyoti.bhaduri@gmail.com, d.bhaduri@bham.ac.uk (D. Bhaduri), p.penchev@bham.ac.uk (P. Penchev), s.s.dimov@bham.ac.uk (S. Dimov), s.l.soo@bham.ac.uk (S.L. Soo).

http://dx.doi.org/10.1016/j.measurement.2016.03.033
0263-2241/© 2016 Published by Elsevier Ltd.

Table 1
Test plan for the conducted comparative study.

Test no.	Test description	Component technologies
1.	Machining of 30 × 30 mm fields with perpendicular intersecting trenches to structure silicon (Si) wafers or stainless steel (SS304) plates. The nominal width and depth of the trenches are 100 and 10 μm respectively while they are 1 mm apart along the *X* and *Y* axes. The test quantifies the positional accuracy of *X*–*Y* scan heads	(1) *X* and *Y* beam deflectors (2) Focusing lens system
2.	The same perpendicular intersecting trenches as in Test 1 are produced on Si wafers or SS304 plates with a stationary beam and moving mechanical axes. The test assesses the accuracy of the *X*–*Y* mechanical stages	(1) *X* and *Y* mechanical stages (2) Focusing lens system
3.	Four 30 × 30 mm fields with perpendicularly intersecting trenches are machined on a 70 × 70 mm area of Si wafers or SS304 plates. The nominal width and depth of the trenches are 200 and 20 μm respectively while they are 1 mm apart from each other in the *X* and *Y* directions. The structuring is carried out using the optical axes only, whereas the repositioning between the fields is carried out using the mechanical axes only. The test is intended to quantify the accuracy of both *XY* scan heads and *XY* mechanical stages	(1) *X* and *Y* beam deflectors (2) *X* and *Y* stages (3) Focusing lens system
4.	Test 1 is repeated after adjusting the beam spot diameter at the focal plane using a beam expander and then calibrating the scan head. The test quantified the effectiveness of the calibration routines after conditioning the beam diameters	(1) *X* and *Y* deflectors (2) Beam expander (3) Calibration routine (4) Focusing lens system
5.	Machining of 30 × 30 mm fields with perpendicular intersecting trenches is performed with different scanning speeds (100, 500 and 1500 mm/s) on stainless steel SS304 plates tilted at 9° along either *X* or *Y* axes. The test is carried out using the optical axes and the *Z* module of the scan heads. The test quantifies the dynamic capabilities of *Z* modules when laser processing 3D surfaces	(1) *X* and *Y* deflectors (2) *Z*-module (3) Focusing lens system
6.	Producing arrays of dimples on SS304 plates that are normal and tilted (at 0°, 5°, 10°, 15° and 20° along *Y*-axis) in regards to the beam. Each dimple is produced with a sequence of 20 pulses on the "fly" (20 passes of the bean) with five scanning speed settings (100, 500, 1000, 1500 and 2000 mm/s) and thus to quantify the combined effect of optical axes and *Z*-module on ARR	(1) *X* and *Y* beam deflectors (2) *Z*-module (3) Focusing lens system

were used successfully in a wide range of measurements and surface characterisation tasks, e.g. for inspecting cast surfaces [12], cutting tool geometry [13], quality of holes in drilling operations [14] and also for quantitative micro morphological analyses of cut marks in bones [15].

Although there were a few publications where the capability of different laser machining platforms were investigated [5], a systematic comparative study of key component technologies of their beam delivery systems were not conducted despite the fact that the accuracy and repeatability of the beam–workpiece relative movements are determined by them. Therefore, the aim of this research was to evaluate the capabilities of state-of-the-art laser processing systems that were specially designed and implemented for laser micro structuring and texturing. A comparative study was conducted to investigate the ARR capabilities of such laser processing setups and thus to quantify the contributions of their key component technologies towards the systems' overall performance. In particular, the component technologies of their beam delivery systems were investigated by conducting an empirical study to quantify and compare ARR of their optical (3D scan heads) and mechanical axes (linear stages) when they were used separately or in different combinations for precision laser surface structuring/texturing.

2. Comparative study design

2.1. Test plan and machine specifications

A sequence of six tests, described in Table 1, was planned in order to assess ARR of optical and mechanical axes of laser machining platforms. The tests were designed to minimise the effects of laser-material interactions on the ARR. In particular, only the relative distances between the trenches were measured while their widths and depth as well as the resulting surface quality were not considered. Four laser micromachining systems were investigated, hereafter denoted as Systems A, B, C and D. A schematic diagram depicting the component technologies is shown in Fig. 1 together with their specifications provided in Table 2. The specimens produced together with their corresponding test numbers are given in Table 3.

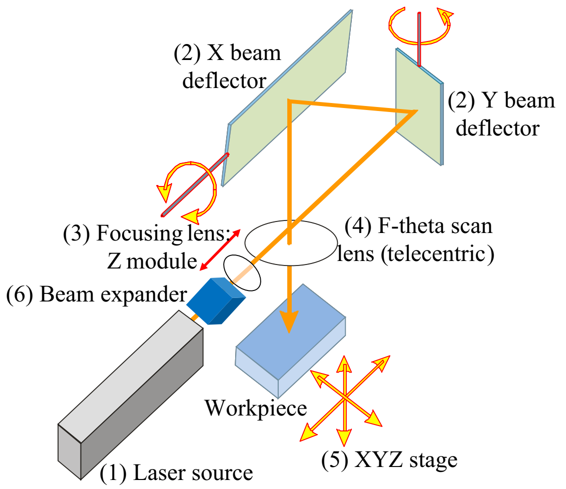

Fig. 1. Schematic diagram showing the component technologies of a laser micromachining system.

The laser processing settings on the four systems were selected by their operators to make the best use of their capabilities and also to achieve the nominal dimensions required in the six tests as stated in Table 1. The optical axes of the four systems were calibrated before carrying out the tests and thus to perform within their technical specifications. In addition, the mechanical stages of the four systems had an interferometer calibration and error mapping of individual axes where micron level linear errors were analysed and the resulting calibration information was included as a look-up table to perform movements with high accuracy and repeatability [16]. It is important to note that the four investigated systems integrate similar and in some cases even identical state-of-the-art representative component technologies, that are equipped with the latest integration tools. Furthermore, the systems were implemented by different integrators in order to assess objectively the effects of key component technologies on laser systems' performance rather than judging about the integration capabilities of any particular integrator.

2.2. Measurement procedure

The measurements on laser structured/textured surfaces were carried out using the FV technology, in particular an Alicona G4 InfiniteFocus microscope. Some preliminary measurements of the machined fields were conducted using four different objectives, in particular 5×, 10×, 20× and 50×. The aim of these measurements was to assess the measurement uncertainties associated with these four objective lenses in context of the planned six tests (see Table 1). A Test 1 structure, as shown in Fig. 2, produced with System A was used to carry out this uncertainty assessment. The area enclosed between 1st and 6th trenches was scanned and the corresponding distances between the trenches was measured. To minimise the effect of laser-material interactions on the trench width, the measurements were taken from the edge of 1st trench to the corresponding edge of 6th trench. The '2D measurement' tool provided by the Alicona data analysis software with capabilities for detecting edges automatically was used and the corresponding uncertainties associated with the measurements were calculated [17]. Three measurements along the edges of 1st and 6th trenches were performed as shown in Fig. 3 by employing the four objective lenses considered in this preliminary study with their respective sets of vertical and horizontal resolutions. The sets of resolutions used for the four objectives were different due to the scanning time associated with the higher magnification lenses, in particular two and one with the 20× and 50× objectives, respectively while five and four for the 5× and 10× objectives. The calculated average values are plotted in Fig. 4. The measurement uncertainty (Type A) was calculated according to Eqs. (1)–(3).

$$s^2 = \frac{\sum_{i=1}^{n}(y_i - \bar{y})^2}{n-1} \quad (1)$$

$$s = \sqrt{\frac{\sum_{i=1}^{n}(y_i - \bar{y})^2}{n-1}} \quad (2)$$

$$u = s \quad (3)$$

where

s^2 – the sample variance;
s – the sample standard deviation;

Table 2
Technical specifications of component technologies (as provided be vendors).

Systems	A		B		C	D	
Beam delivery system							
XY scanning head							
Max scanner speed (*XY*)	25 rad/s		25 rad/s		2 m/s with 160 mm focusing lens system	–	
Pos. resolution (μ rad)	<12		<12		10	<8	
Thermal drift (μ rad)	<±12		<±12		<25	<20	
Tracking error (μs)	110		110		110	<20	
Focusing lens system							
Focal length (mm)	100	160	100	160	160	100	163
Focusing field (mm)	35 × 35	60 × 60	35 × 35	80 × 80	100 × 100	35 × 35	80 × 80
Beam spot size (μm)	30	60	20–56	20–90	40	20–56	40–90
Z-module							
Focusing range (mm)	6	10	6	10	–	10	
Mechanical axes							
XY axes/stage							
Travel (mm)	300		300 × 300		160	600 × 450	
Max.travel speed (mm/s)	500		500		300	500	
Resolution (μm)	0.25		0.25		0.01	1.0	
Accuracy per axis (μm)	±2		±2		±0.75	±0.5	
XY Accuracy (2D) (μm)	±4		±4		–	±1.0	
Z axis/stage							
Travel (mm)	300		300		300	200	
Max.travel speed (mm/s)	50		50		10	220	
Resolution (μm)	0.5		0.5		0.1	1.0	
Accuracy per axis (μm)	±1		±1		±0.75	±1.0	
XY Accuracy (complete 2D travel) (μm)	±10		±10		–	±10	

Please cite this article in press as: D. Bhaduri et al., An investigation of accuracy, repeatability and reproducibility of laser micromachining systems, Measurement (2016), http://dx.doi.org/10.1016/j.measurement.2016.03.033

Table 3
Samples produced on the four different laser systems.

Laser systems	Test no. 1	2	3	4	5	6
A	×	×	×		×	×
B	×	×		×		
C	×		×	×		
D	×	×	×	×		

n – the number of measurements;
$\bar{y}$ – the average of n measurements;
$\bar{y} = \frac{\sum_{i=1}^{n} y_i}{n}$
u – standard uncertainty for Type A evaluation.

As expected, uncertainty decreased from 1.54 µm to 0.15 µm as the magnification increased from 5× to 50×. Although these values were within 10% of the accuracy of the beam delivery system, i.e. ±10 µm, aimed in this research, the edge detection on the 3D scanned images required the use of 20× and 50× objectives. Especially, the higher magnifications were used to minimise the effects of different edge definitions obtained by applying different laser processing settings and laser sources on the four investigated systems. A 50× magnification was used only for inspecting the Tests 2 and 3 specimens due to the high ARR aimed at with the use of mechanical stages, i.e. ±2 µm; whereas a 20× magnification was utilised for the Tests 1, 4 and 5 where scan heads were employed with an objective to achieve an accuracy of ±10 µm. The vertical resolution of the 20× was doubled from 0.205 µm (used in the preliminary study, see Fig. 3) to 0.41 µm in order to reduce the measurement time while the lateral resolution was kept unchanged at 1.76 µm. For the 50× objective, a slightly lower vertical resolution of 0.30 µm (instead of 0.205 µm in Fig. 3) was utilised but a higher lateral resolution (0.80 µm) was employed to obtain better edge detection.

For Tests 1, 2, 4 and 5, the measurements were carried out at the two diagonally opposite corners of the structured fields as the lowest accuracy of the beam deflectors were expected there while the highest in the centre of the scan fields. In particular, the 20× magnification was used to scan the areas between the 1st and 11th trenches in Tests 1, 4 and 5 and also to measure the distances between 1st and 3rd, 1st and 5th, 1st and 7th, 1st and 9th and 1st and 11th trenches along both horizontal (X-axis) and vertical directions (Y-axis). A similar measurement procedure was applied in Test 2, however only the distances from 1st to 2nd, 3rd, 4th and 5th trenches were measured due to the large size of the scan data generated with the 50× objective. The schematic diagrams of the measured regions in Tests 1, 2, 4 and 5 are depicted in Fig. 5(a) and (b). The positional accuracies of the beam deflectors and the stages of the four laser micromachining systems analysed in this comparative study were then determined by comparing the nominal values with the measurement results.

A representative 3D image of a scanned region on a Test 1 specimen is shown in Fig. 6(a) while the top view is shown in Fig. 6(b). The point data from the scans were analysed using the 'Profile form measurement' tool available in the Alicona software. The data were treated with 'form' removal operation prior to measuring the distances between trenches. The edge of the 1st trench in Tests 1, 4 and 5 was used as a datum for measuring the distances to the corresponding edges of the 3rd and similarly 5th, 7th, 9th and 11th trenches using the software tool. Ten lateral measurements were taken for each scanned area as illustrated in Fig. 6 and the average values were calculated.

The measurements in Test 3 were carried out along the horizontal (X) and vertical (Y) axes at the stitching junction of the laser scanned fields as it is schematically shown in Fig. 7(a). The procedure is detailed in Fig. 7(b) that included measuring the distances from 1st to 2nd, 3rd, 4th and 5th trenches. The D_1 and D_2 measurements provide information about the accuracy of the beam deflectors when structuring Field 1 while D_4–D_3 renders equivalent information about Field 2. At the same time, D_3–D_2 provides information about the accuracy of the stage as the mechanical axes were used to reposition the laser processed areas from Field 1 to Field 2.

Furthermore, D_2–D_1 and D_4–D_3 measurements provide information about the pseudo-repeatability of laser structuring operation carried out only with the beam deflectors,

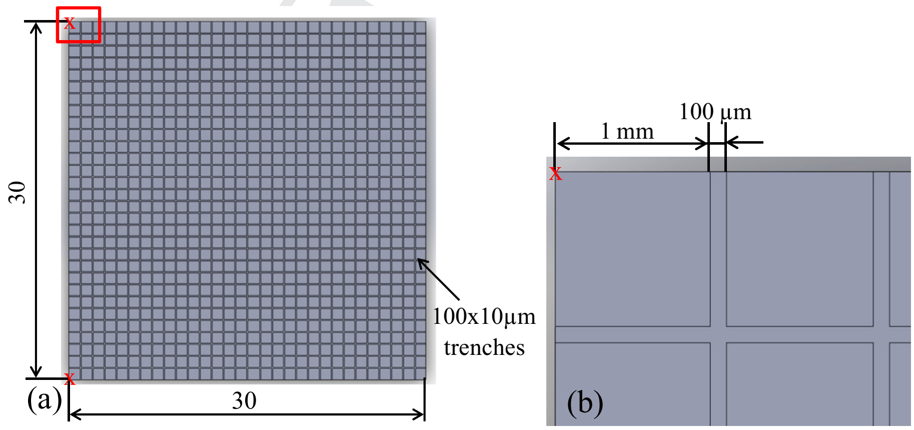

Fig. 2. (a) The 30 × 30 mm field machined with System A, and (b) nominal distance between two consecutive trenches.

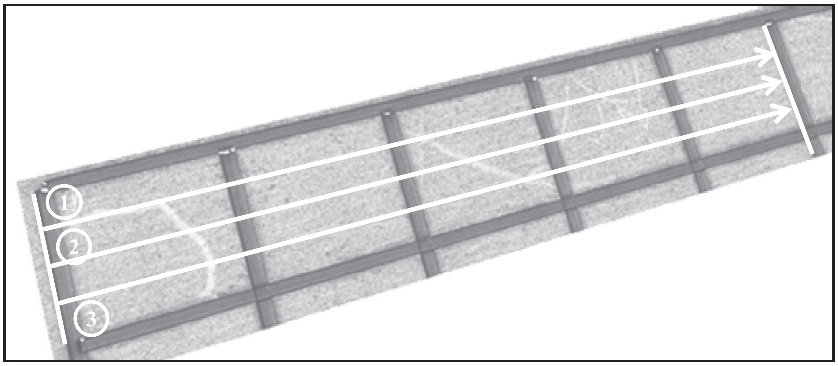

Fig. 3. Three measurements of the distance between the 1st and 6th trenches.

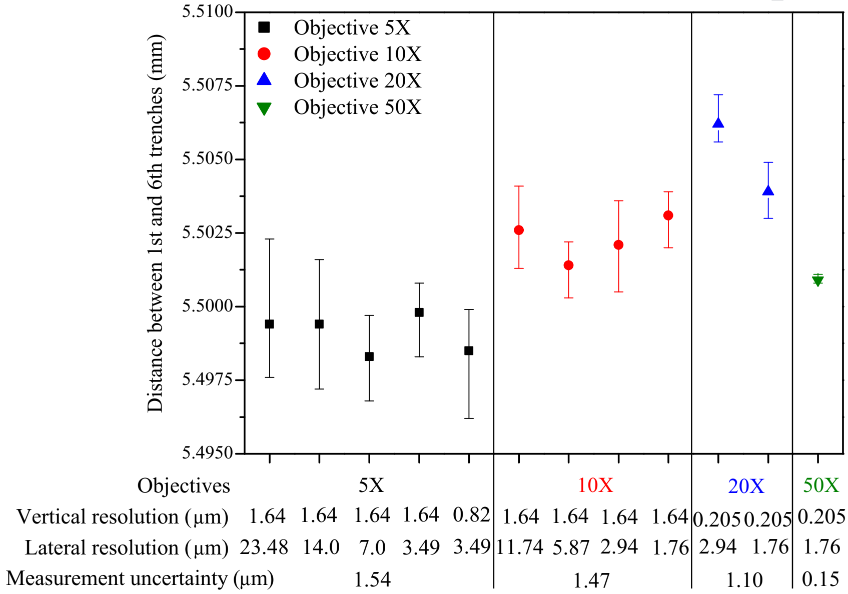

Fig. 4. Plot of the average values measured with four objective lenses.

while D_2 and the distance from the 1st to 3rd trenches in Test 1 exhibit reproducibility of structuring operations, i.e. the machining precision obtained with the beam deflectors [5].

Test 6 involved measuring the depths and diameters of the dimples produced at various scanning speeds using the 'Profile form measurement tool'. A representative scanned area of the dimples together with the measured depth and diameter is shown in Fig. 8.

3. Results and discussion

3.1. Tests 1 and 4

The results obtained in Test 1, i.e. by using the *X*-axis beam deflectors, are shown in Fig. 9. The positional accuracy typically decreased with the increase of the distance from the 1st trench. System A achieved the best accuracy amongst the four systems with values between 0.76 and 12.74 μm while the majority of data was within the technical specification for the optical axes, i.e. ±10 μm, whereas positional errors of the other three micromachining set-ups was much higher. System C exhibited the worst results, i.e. deviations up to ∼300 μm, followed by the System B and System D. The positional accuracy between the corners 1 and 2 of Systems B and D was in the range from 2 to 40 μm.

The graph in Fig. 10 shows that the accuracy of System A along the *Y*-axis was again the best amongst all four systems, however with a marginally higher deviation, up to 15.65 μm, in comparison to that along the *X*-axis. Conversely, System B exhibited greater deviation in *X*, up to 120 μm, compared to that in *Y* axis, up to −65 μm. The results obtained with System C were the worst among all set-ups with values gradually increasing from the 1st to 11th trenches and this can be attributed to a systematic error in carrying out laser machining operations. The accuracy of System D's optical axes was similar along both axes.

Please cite this article in press as: D. Bhaduri et al., An investigation of accuracy, repeatability and reproducibility of laser micromachining systems, Measurement (2016), http://dx.doi.org/10.1016/j.measurement.2016.03.033

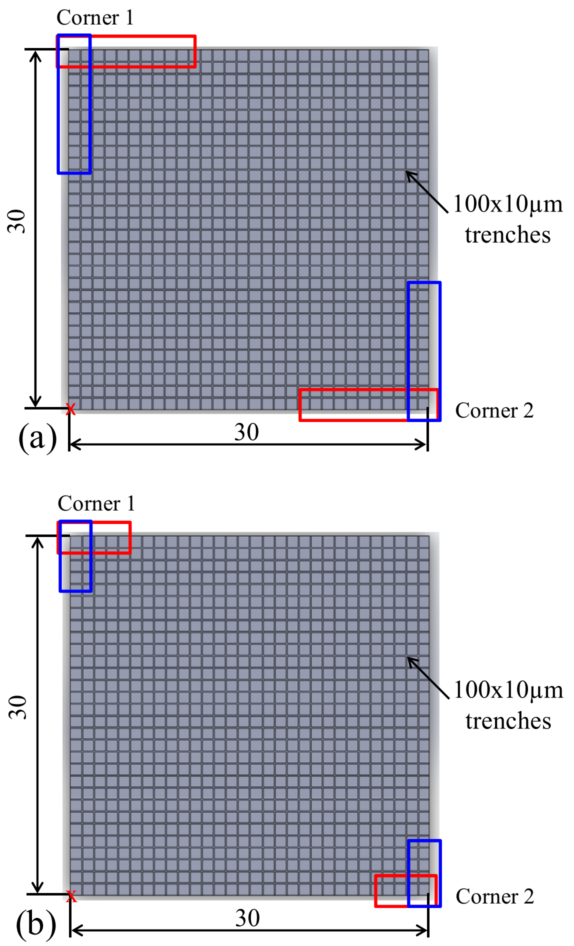

Fig. 5. Scanned regions for (a) Tests 1, 4 and 5, and (b) Test 2.

The positional accuracy of the beam delivery systems improved typically when the systems were calibrated after using the beam expanders. Positional accuracy of System D improved by ~75–93%, with values from 1.22 to 11.25 µm along *X* (Fig. 11), and ~35–45% in *Y* (Fig. 12). Thus, regular calibrations of the beam delivery systems are very important, especially if precision laser machining operations have to be performed. Typically, a positive systematic error was noted for System D in *X* as opposed to a negative along *Y*. Systems B and C however did not show any significant improvements, possibly due to the calibration errors associated with both machines, although the accuracy in *X* was marginally better for System C.

3.2. Test 2

As expected, the accuracy of the mechanical stages was much better, typically in the range of ±2–4 µm, than their optical counterpart. This is due partly to the much lower processing speed, typically less than 100 mm/s, compared to the optical axes, which operate at speeds higher than 1 m/s when texturing/structuring operations are performed. The deviation from the nominal value generally increased with the distance from the 1st trench as shown in Fig. 13. Systems A and B performed better in *X* than in *Y*; while for System D the accuracy was comparable in both directions as depicted in Fig. 14.

3.3. Test 3

The position accuracy of the System A's beam deflector along the *X*-axis varied from 2.84 to −5.81 µm as shown in Table 4 while that of mechanical axes was within −1.02 to −1.91 µm; however, both were within the system's technical specifications of ±10 and ±4 µm, respectively. Con-

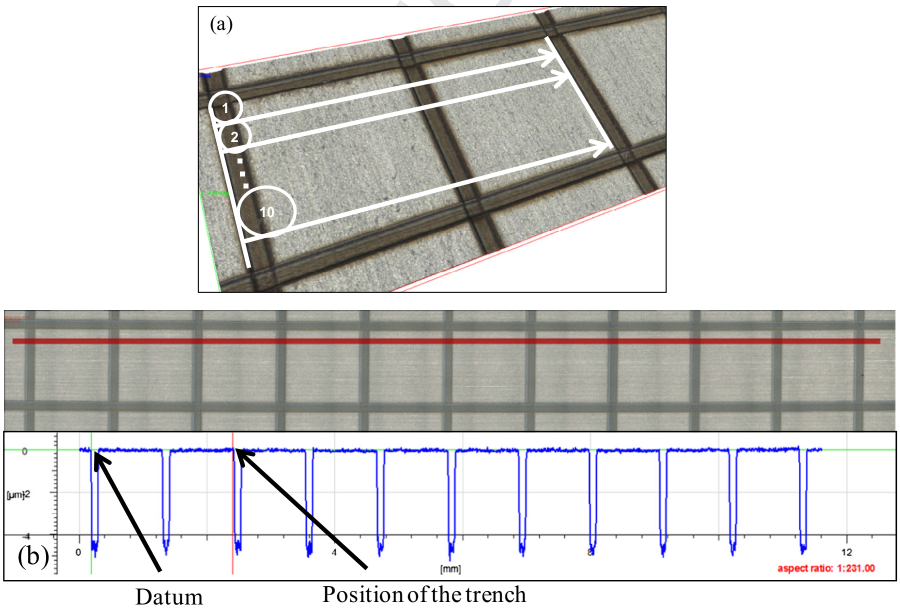

Fig. 6. (a) Ten measurements on laser scanned area, and (b) measurement of distances between the trenches using 'Profile form measurement' tool.

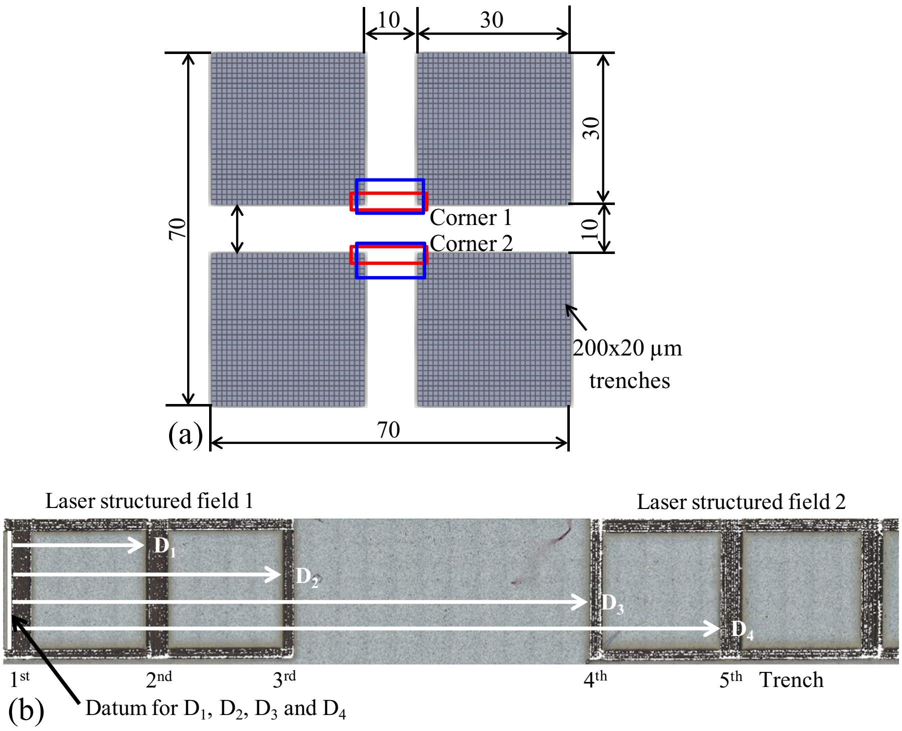

Fig. 7. (a) Schematic diagram of the four structured fields in Test 3, and (b) measurement procedure in Test 3.

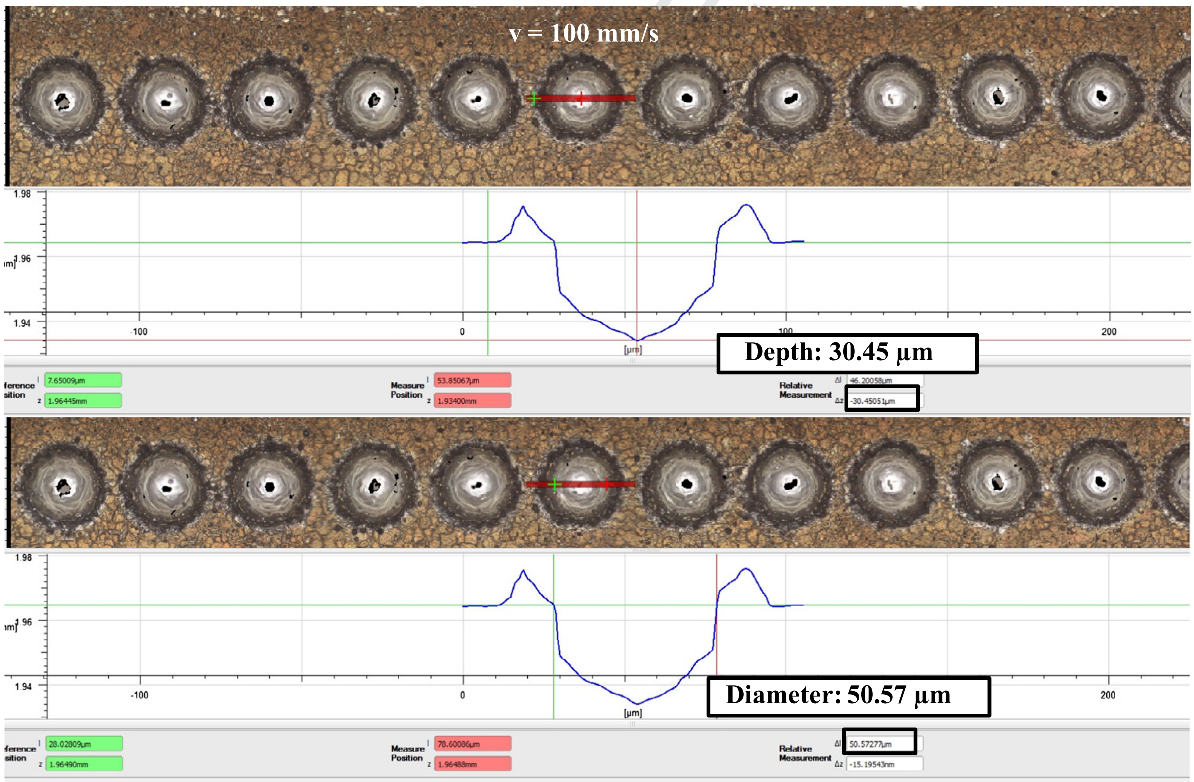

Fig. 8. A scanned area containing several dimples created at various scanning speeds together with the measured depth and diameter of one of them.

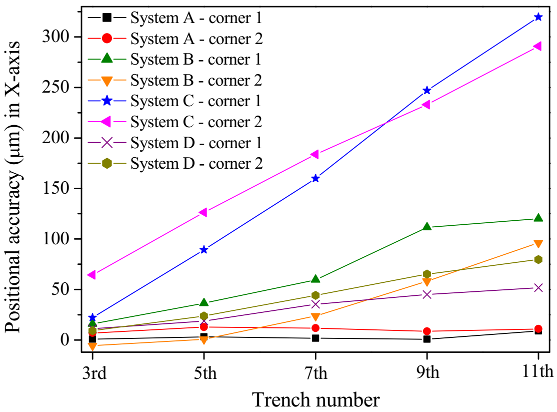

Fig. 9. Positional accuracy of beam deflectors along the *X*-axis in Test 1.

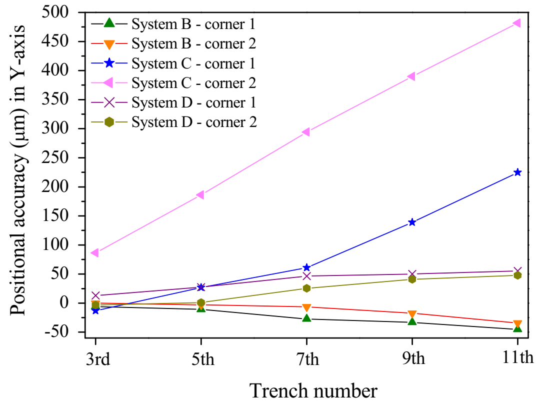

Fig. 12. Positional accuracy of beam deflectors along the *Y*-axis in Test 4.

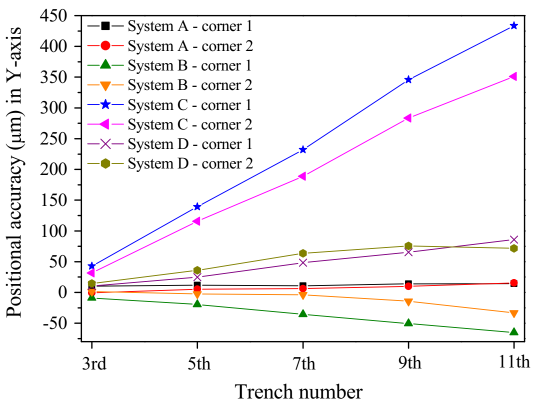

Fig. 10. Positional accuracy of beam deflectors along the *Y*-axis in Test 1.

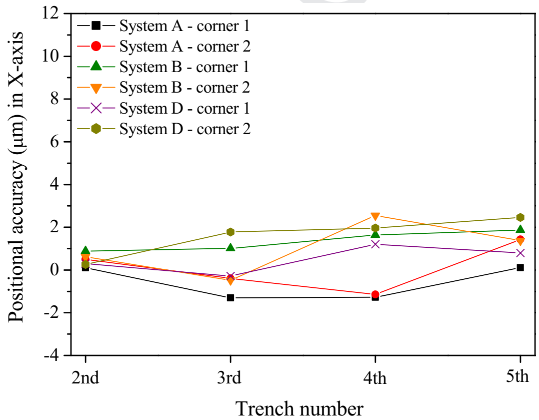

Fig. 13. Positional accuracy of mechanical axes along the *X*-axis in Test 2.

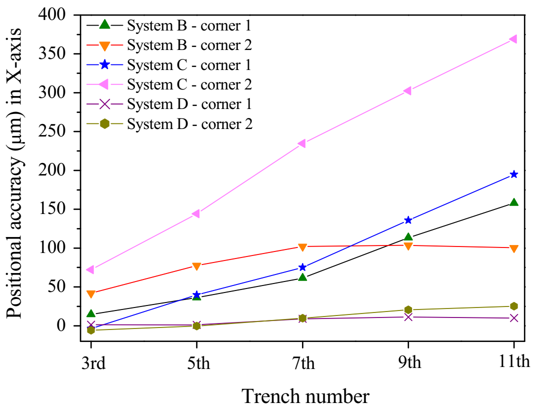

Fig. 11. Positional accuracy of beam deflectors along the *X*-axis in Test 4.

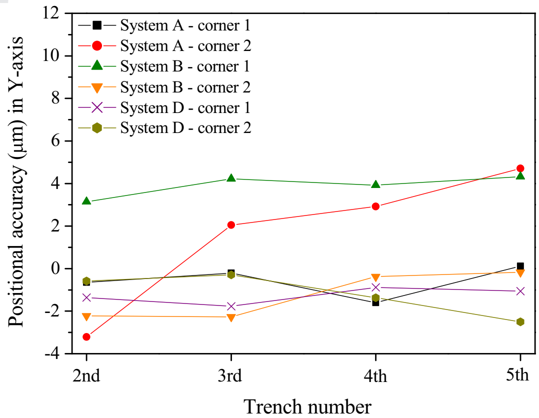

Fig. 14. Positional accuracy of mechanical axes along the *Y*-axis in Test 2.

versely, the deviations of the scanners were much higher for Systems C and D. As it was already mentioned, this was possibly due to calibration issues for both set-ups. Although the accuracy of the mechanical axes of both systems at Corner 1 was 2.72 and −2.02 µm respectively, that at Corner 2 was much lower, −15.08 and 14.70 µm for Systems C and D. The deviations of the mechanical stages were still typically lower than that of the scanners, which can be explained with the scanners' much higher processing speeds.

The stitching accuracy of the machined fields along the *Y*-axis was measured only for System A due to the time constraints. Better stitching accuracy was observed at

Table 4
Positional accuracies of the scan heads and mechanical stages along *X* in Test 3.

Systems	Corner	Field 1 (D_2–D_1) (μm)	Field 2 (D_4–D_3) (μm)	Mechanical axes (D_3–D_2) (μm)
A	1	−4.74	3.17	−1.91
	2	−5.81	2.84	−1.02
C	1	63.74	69.92	2.72
	2	58.62	71.96	−15.08
D	1	12.46	54.06	−2.20
	2	11.78	51.74	14.70

Table 5
Stitching accuracy along the *Y*-axis in Test 3.

System A	Stitching accuracy (μm)				
	1st trench	2nd trench	3rd trench	4th trench	5th trench
Corner 1	0.70	3.52	2.42	2.64	2.64
Corner 2	−6.46	−8.12	−8.32	−8.94	−11.0

Corner 1 compared to that at Corner 2 with values ranging from 0.70 to 2.64 and −6.46 to −11 μm, respectively as shown in Table 5.

3.4. Test 5

The positional accuracies of System A's scan head when structuring inclined surfaces either along *X* or *Y*-axis are shown in Figs. 15–18. The deviation from the nominal values in *X*-axis greatly increased from 14 to 108 μm when the surface was inclined along the same axis, whereas positional accuracy along the *Y* varied only from ~5 to 32 μm. Similar results were also observed when the plate was inclined along *Y*-axis. In this case, the accuracy along the *X*-axis was within 1.5–10 μm while that along *Y* varied from ~30 to 190 μm. It was further noticed that the accuracy of *X*-axis was typically better compared to that of *Y*. This was in line with the observation from Test 1 on System A's scan head accuracy.

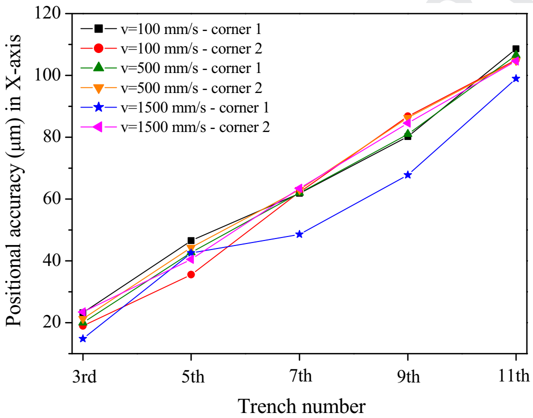

Fig. 15. Positional accuracies along the *X*-axis in Test 5 (workpiece inclined along *X*-axis).

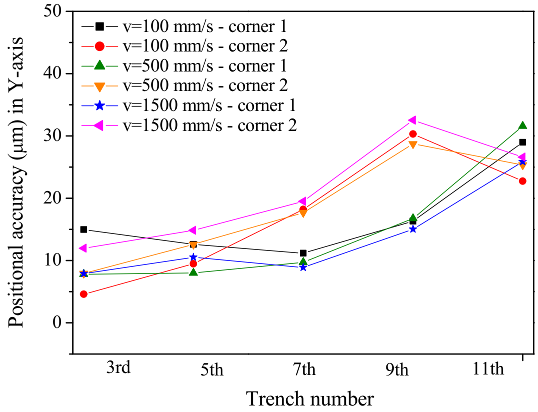

Fig. 16. Positional accuracies along the *Y*-axis in Test 5 (workpiece inclined along *X*-axis).

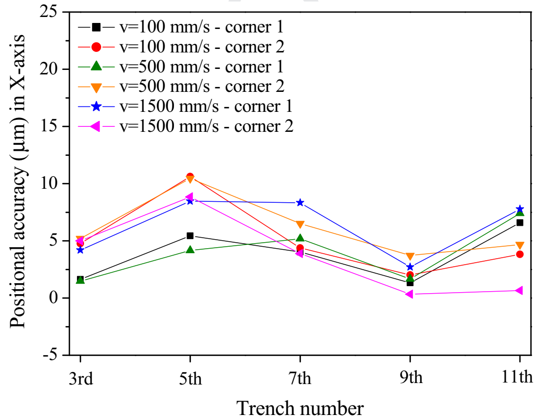

Fig. 17. Positional accuracies along the *X*-axis in Test 5 (workpiece inclined along *Y*-axis).

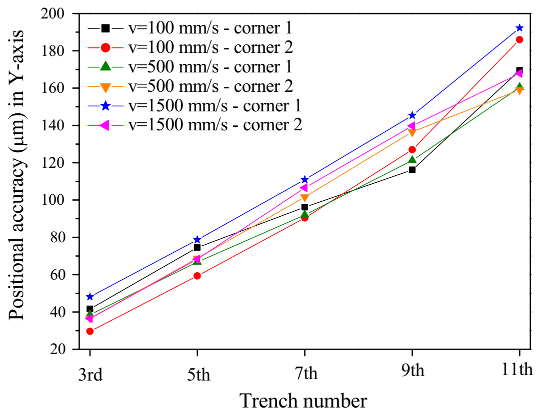

Fig. 18. Positional accuracies along the *Y*-axis in Test 5 (workpiece inclined along *Y*-axis).

The accuracy deterioration in Test 5 can be attributed to 3D calibration errors. For example, greater errors were observed in Figs. 15 and 16 along the inclined *X*-axis, where each of the trenches was produced with a constant *Z*-module focusing settings. This is illustrated in Fig. 19, where no programmed movements occurred in the *Z* direction; thus the dynamic capabilities of the *Z*-module should not affect the trenches' positional accuracy. Similarly, bigger positional errors were observed in Figs. 17 and 18 along the inclined *Y*-axis, where trenches were again produced without any movements along the *Z*-axis. Although Figs. 16 and 18 exhibit that the accuracy slightly deteriorated with the increase of laser scanning speed for the trenches requiring programmed movements along the *Z*-axis, this does not provide any conclusive evidences regarding the *Z*-module's performance in comparison to the *X* and *Y* beam deflectors.

3.5. Test 6

The depths and diameters of the dimples produced on surfaces normal and inclined to the incident beam are shown in Figs. 20 and 21, respectively. With the increase of the scanning speed, dimple depths remained typically consistent within the range of 27–29 μm on the sample normal to the incident beam. Similar results were also obtained on the sample when inclined at 5° and 10°. However with the increase of the inclination angle (greater than 10°), the dimple depths decreased gradually with the increase of the scanning speed. This could be attributed to the lower *Z*-module dynamics that led to a lag in executing the programmed focusing movements along the *Z*-axis and consequently affected the machining results. The negative effects were more pronounced at the higher inclination angles, i.e. 15° and 20° where the depth of the focus (approximately 2.45 mm with the used beam delivery configuration) could not compensate the inferior dynamics of the *Z*-module compared with that of the *X* and *Y* beam deflectors. In particular, these negative effects on the dimple depths are clearly observed at scanning speeds higher than 1 m/s when the samples were inclined at 15° and 20° (see Fig. 20). For example, the dimple depths at a scanning speed of 2 m/s have been reduced to 25.5 μm and 19.5 μm at the inclination angles of 15° and 20°, respectively. This statement regarding the *Z*-module's performance is supported by the carried out Analysis of Variance (ANOVA) in Table 6. In particular, ANOVA shows that the inclination angle (θ) had the highest contribution of 56.97% on the dimple depth, followed by an interaction of scanning speed (v) and θ and the sole of effect of v, i.e. 30.53% and 12.50% respectively.

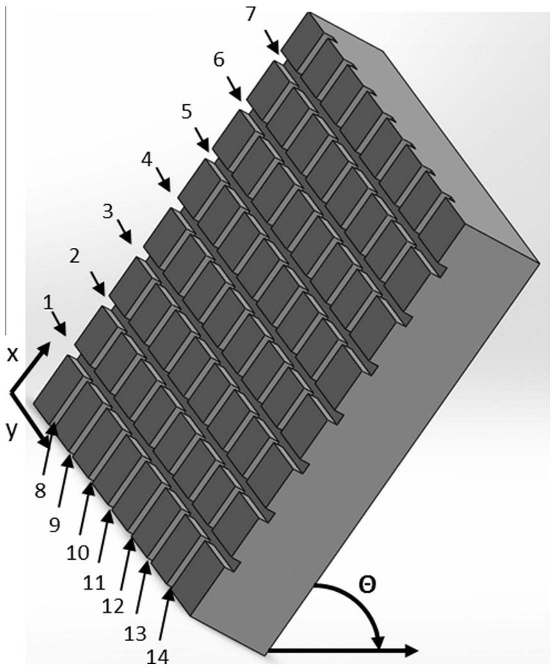

Fig. 19. Graphical representation of trenches produced along the inclined *X*-axis. *Note:* when producing the trenches normal to the *X*-axis, the *Z*-module is fixed at a certain *Z* setting throughout the machining of the trenchs, while the *Y* beam deflector executes the machining movements. In contrast, when producing the trenches normal to the *Y*-axis both the *X* beam deflector and the *Z*-module simultaneously execute the machining movements.

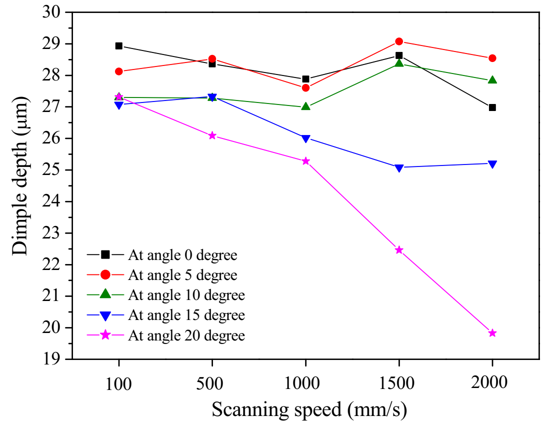

Fig. 20. The plot of dimple depth produced on normal and inclined surfaces to the incident beams at various scanning speeds in Test 6.

The diameters of the dimples, as shown in Fig. 21, gradually increased with the increase of scanning speed at all investigated inclination angles. Conversely, dimple diameters decreased with the increase of the angle at the lower processing speeds, i.e. 100 mm/s and 500 mm/s, however such a trend was not apparent at the higher scanning speeds, i.e. 1 m/s and 1.5 m/s. The increase of dimple diameter with the increase of processing speed is also clearly depicted in Figs. 22 and 23. This can be explained with the deterioration of dimples' positional accuracy due to the lower *Z*-module dynamics compared with the *X* and *Y* beam deflectors. Especially, this results in shifting of pulses' incident positions that leads to an increase of the dimple diameters. This is supported by the Analysis of Variance (ANOVA) for dimple diameters in Table 7. In particular, the ANOVA results show that scanning speed was the significant influencing factor for the diameter increase with a PCR of 85.35% while inclination angle and the interaction of v and θ had PCRs of 6.58% and 8.07%, respectively.

Based on the results for dimple diameters and depths in Test 6, it can be stated that the depth of focus could not

Please cite this article in press as: D. Bhaduri et al., An investigation of accuracy, repeatability and reproducibility of laser micromachining systems, Measurement (2016), http://dx.doi.org/10.1016/j.measurement.2016.03.033

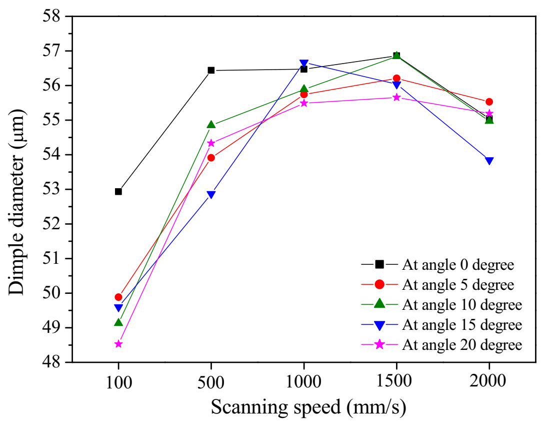

Fig. 21. The plot of dimple diameters produced on normal and inclined samples to the incident beam at various scanning speeds in Test 6.

compensate completely the inferior *Z*-module dynamic at higher inclination angles and scanning speeds. Thus, it is necessary to investigate the *Z*-modules' dynamic performance and its potential negative impact on 3D laser machining results. An experimental technique to conduct such investigation is reported in another study [18].

3.6. Repeatability and reproducibility

Pseudo-repeatability data of Systems A, C and D are presented in Table 8. It compares the distance between 1st and 2nd trenches within the laser structured Fields 1 and 2 in Test 3. Systems A and C exhibited a pseudo-repeatability in the range of 6.18–13.34 µm at the two corners of the machined fields. However, pseudo-repeatability of the System D was much worse (in the range of 39.96–

Table 6
Analysis of variance for dimple depths in Test 6.

Source	Degrees of freedom	Sum of squares	Mean squares	$F_{calculated}$	$F_{tabulated}$	Percentage contribution ratio (PCR)
Scanning speed (v)	4	13.22	3.31			12.50
Angle of inclination (θ)	4	60.27	15.07	4.55	6.38	56.97
$v \times \theta$	16	32.30	2.02	0.61	5.84	30.53
Error	0					
Pooled error	4	13.22	3.31			
Total	24	105.79				100.00

At 95% confidence level.

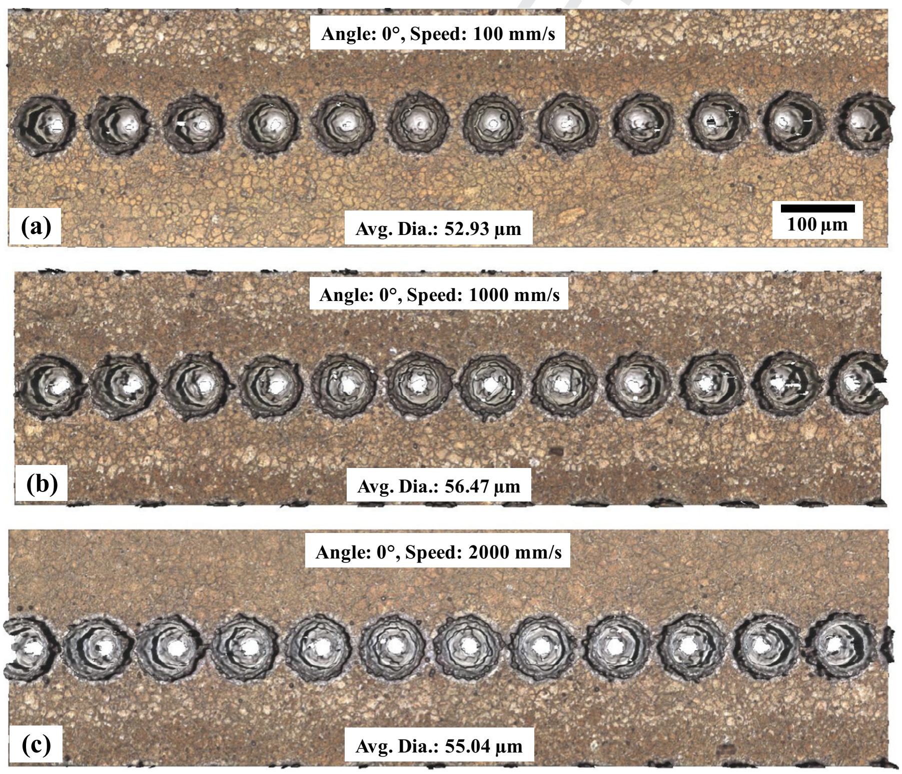

Fig. 22. Scanned images of dimples produced on a surface normal to the incident beam at three different scanning speeds: (a) 100, (b) 500 and (c) 1500 mm/s.

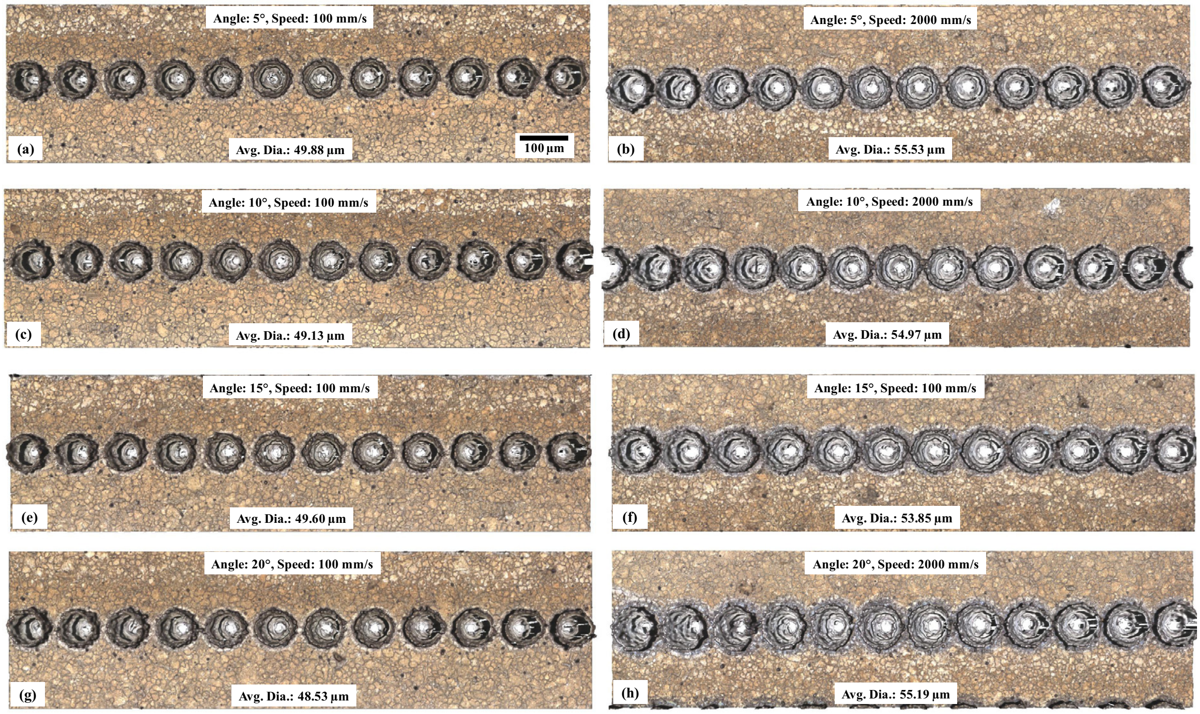

Fig. 23. The dimples produced with two scanning speeds on the samples inclined to the incident beam at four different angles.

Table 7
Analysis of variance for dimple diameters in Test 6.

Source	Degrees of freedom	Sum of squares	Mean squares	$F_{calculated}$	$F_{tabulated}$	Percentage contribution ratio (PCR)
Scanning speed (v)	4	129.66	32.42	12.97*	3.01	85.35
Angle of inclination (θ)	4	9.99	2.50	0.31	3.01	6.58
$v \times \theta$	16	12.27	0.77			8.07
Error	0					
Pooled error	16	9.99	2.50			
Total	24	151.92				100.00

At 95% confidence level.
* Statistically significant.

Table 8
Pseudo-repeatability data of different laser systems.

Systems	Regions	Test 3		Repeatability (µm)
		Field 1 Accuracy (µm)	Field 2 Accuracy (µm)	
A	Corner 1	−4.74	3.17	8.44
	Corner 2	−5.81	2.84	8.65
C	Corner 1	63.74	69.92	6.18
	Corner 2	58.62	71.96	13.34
D	Corner 1	12.46	54.06	41.60
	Corner 2	11.78	51.74	39.96

41.60 µm), although the results within each field (Corners 1 and 2) were comparable.

The reproducibility of the optical axes of Systems A, C and D was determined by comparing the distance between 1st and 3rd trenches in Tests 1 and 3 as shown in Table 9. The results obtained solely with the scan heads were reproducible and ranged from 1 to 6 µm with only two exceptions.

Please cite this article in press as: D. Bhaduri et al., An investigation of accuracy, repeatability and reproducibility of laser micromachining systems, Measurement (2016), http://dx.doi.org/10.1016/j.measurement.2016.03.033

Table 9
Laser scanheads' reproducibility of Systems A, C and D.

Systems	Regions	Test 1 Deviation from the nominal (μm)	Test 3 Deviation from the nominal (μm)	Reproducibility (Precision) (μm)
A	Corner 1	0.76	−4.74	5.50
	Corner 2	6.94	−5.81	12.75
C	Corner 1	22.20	63.74	41.54
	Corner 2	64.48	58.62	−5.86
D	Corner 1	11.31	12.46	1.15
	Corner 2	9.13	11.78	2.65

4. Conclusions

The following conclusions can be made based on the carried out comparative study:

- The accuracy of the optical axes typically decreased with the increase of nominal dimensions; however, it should be noted that some systematic measurement errors could have contributed to these results. At the same time, the tests have shown that the calibration of scan heads is very important and can substantially improve the positional accuracy. Frequent calibrations are essential for obtaining the desired level of machining accuracy, especially when any modifications in the optical beam delivery configurations are made. Other factors affecting the calibration include environmental factors such as temperature, humidity and vibration, as they can influence the laser beam pointing stability and deteriorate the machining accuracy.
- The accuracy of the mechanical axes was much better, generally in the range of ±2–4 μm, compared to that of the optical axes. This could be partially attributed to the much lower processing speed of the mechanical stages, typically less than 100 mm/s, in contrast to that of the scan heads, greater than 500 mm/s.
- The lower dynamics of *Z*-module affected the positional accuracies of the beam delivery system when processing inclined surfaces at different scanning speeds. The deviation from the nominal value increases with the increase of scanning speeds. Only at relatively lower scanning speeds, the depth of focus can compensate the inferior dynamics of *Z*-module to some extent, in comparison to *X* and *Y* beam deflectors.
- Although the dimple depths were consistent when produced on a surface normal to the incident beam, their diameters increased at higher processing speeds. In contrast, dimple depths decreased with the increase of inclination angles. This can be attributed to the lower *Z*-module dynamics that affected the processing efficiency.
- Although two of the systems produced repeatable results with their scan heads, this was not the case for the other system analysed in this study. However, all systems were typically capable of rendering reproducible results, i.e. achieving the expected precision with their scan heads.

Acknowledgements

The research was supported by two EC-funded projects, "High Performance Production Line for Small Series Metal Parts" (HYPROLINE) funded by the FP7 NMP programme (Grant Number 314685) and "ECO-efficient LASER technology for FACTories of the future" (ECO-LASERFACT) funded by INTERREG IVB NWE, and a project funded by the Korean Government on "Laser-Based Modules for Functional Surface Texturing".

References

[1] K. Ehmann, Texturing at the nano/micro-scale over large areas, in: NSF CMMI Engineering Research and Innovation Conference, January 4, 2011.
[2] A. Greco, S. Raphaelson, K. Ehmann, Q.J. Wang, C. Lin, Surface texturing of tribological interfaces using the vibromechanical texturing method, J. Manuf. Sci. Eng. 131 (2009) 06105.
[3] Y. Gao, B. Wu, Y. Zhou, S. Tao, A two-step nanosecond laser surface texturing process with smooth surface finish, Appl. Surf. Sci. 257 (2011) 9960–9967.
[4] P.G. Engleman, A. Kurella, A. Samant, C.A. Blue, N.B. Dahotre, The application of laser-induced multi-scale surface texturing, Surf. Eng., JOM (2005) 46–50.
[5] B. Daemi, L. Mattsson, Performance evaluation of laser micromachining installations, in: Proceeding of the 10th International Conference on Multi-Material Micro Manufacture, 2013, pp. 114–117.
[6] D. Mills, T. Kreouzis, A. Sapelkin, B. Unal, N. Zyuzikov, K.W. Kolasinski, Surface texturing of Si, porous Si and TiO_2 by laser ablation, Appl. Surf. Sci. 253 (2007) 6575–6579.
[7] L.M. Vilhena, M. Sedlaček, B. Podgornik, J. Vižintin, A. Babnik, J. Možina, Surface texturing by pulsed Nd:YAG laser, Tribol. Int. 42 (2009) 1496–1504.
[8] W. Yi, X. Dang-Sheng, The effect of laser surface texturing on frictional performance of face seal, J. Mater. Proc. Technol. 197 (2008) 96–100.
[9] J. Li, D. Xiong, H. Wu, Y. Zhang, Y. Qin, Tribological properties of laser surface texturing and molybdenizing duplex-treated stainless steel at elevated temperatures, Surf. Coat. Technol. 228 (2013) S219–S223.
[10] T. Hu, L. Hu, Q. Ding, Effective solution for the tribological problems of Ti–6Al–4V: combination of laser surface texturing and solid lubricant film, Surf. Coat. Technol. 206 (2012) 5060–5066.
[11] S.M. Bello, New results from the examination of cut-marks using three-dimensional imaging, Dev. Quat. Sci. 14 (2011) 249–262.
[12] U.C. Nwaogu, N.S. Tiedje, H.N. Hansen, A non-contact 3D method to characterize the surface roughness of castings, J. Mater. Proc. Technol. 213 (2013) 59–68.
[13] T.Y. Lim, M.M. Ratnam, Edge detection and measurement of nose radii of cutting tool inserts from scanned 2-D images, Opt. Lasers Eng. 50 (2012) 1628–1642.
[14] Pilný Lukáš, L. De Chiffre, M. Píška, M.F. Villumsen, Hole quality and burr reduction in drilling aluminium sheets, CIRP J. Manuf. Sci. Technol. 5 (2012) 102–107.

[15] S.M. Bello, S.A. Parfitt, C. Stringer, Quantitative micromorphological analyses of cut marks produced by ancient and modern handaxes, J. Archaeol. Sci. 36 (2009) 1869–1880.

[16] Industrial Technology Newsletter by Aerotech, High speed, sub-micron positioning, <http://www.industrialtechnology.co.uk/products–high-speed-sub-micron-positioning.html?thread=No> (accessed 07.03.16).

[17] Alicona InfinteFocus Technology brochure, <http://www.alicona.com/home/fileadmin/alicona/pdfs/InfiniteFocusG5_System_and_technical_specification_E.pdf> (accessed 07.03.16).

[18] P. Penchev, S.S. Dimov, D. Bhaduri, Experimental investigation of 3D scanheads for laser micro-processing, Opt. Laser Technol. 81 (2016) 55–59.

Please cite this article in press as: D. Bhaduri et al., An investigation of accuracy, repeatability and reproducibility of laser micromachining systems, Measurement (2016), http://dx.doi.org/10.1016/j.measurement.2016.03.033